Conceptual Design and Performance Analysis of the

Extended Q-range, High Intensity, High Precision Small Angle Diffractometer

FOR SNS

Jinkui Zhao

Spallation Neutron Source

IS-1.1.8.2-6036-RE-A-00

May 2000

Contents

Overview

The High Power Target Station of SNS offers a great opportunity for a world-class Small Angle Scattering Instrument. Besides the high useable flux such an instrument will have, the wide Q-coverage will be *unmatched* by any other SANS instruments. With the use of high angle detectors and Soller collimators, the SANS instrument will have a maximum dynamic Q-range of close to 5000. The high wavelength resolution (or precision) of the spallation source make it possible for the SANS instrument to be used as a medium-resolution diffractometer. The small angle scattering community, as represented by the SANS Instrument Advisory Team, believes that such an instrument with combined small angle scattering and large angle diffraction capabilities will not only serve many of the community's needs today *but also* will open many exciting opportunities for new science. An example is the study of protein-membrane interactions, where protein signals appear at low-Q while lipid signals show up at high-Q (K. He et al, *Biophys. J.* 64,157,1993). Other applications include engineering materials, where simultaneous monitoring of domain small angle scattering and crystal diffraction is of great interest.

This document describes the proposed Extended Q-Range, High Intensity, High Precision Small Angle Diffractometer at SNS, herein referred to as Extended-Q SANS.

Design Goals

The Extended-Q SANS will have the following features:

It will have extended Q-range. The smallest accessible Q-value* will be 0.004$Å^{-1}$ when pinhole geometry is used and 0.001 $Å^{-1}$ when Soller collimators are used. The largest accessible Q-value will be 12 $Å^{-1}$.
It will have high precision. The wavelength resolution, $\delta\lambda/\lambda$ will be <1 %.
It will have high intensity. The available flux at sample position with all configurable collimation lengths will be comparable to or better than any existing SANS instruments.

Design Parameters and Choices

The schematic setup of the Extended-Q SANS is shown in Figure 1. Table 2 summarizes its design and performance parameters. The design choices are fully supported by the SANS Instrument Advisory Team, represented by its executive committee and spokespersons. It has also been fully endorsed by the soft matter breakout session at the SNS Users Meeting in May 2000.

Machine Length

To have the highest useable flux, the instrument has to be as short as possible. The shortest machine length is limited by the angle separation of 13.8° and the shielding requirements between two adjacent beamlines. The total length for the Extended-Q SANS is chosen at 18m,

* $Q = (4\pi/\lambda)\sin(\theta)$, where λ is the wavelength of neutrons, 2θ is the scattering angle.

with sample at 14m[†] and a maximum sample to detector distance of 4m. At the sample position, the tangential beamline separation will be ~ 3.36m. Taking into account the ~48 cm beam bending (through the use of beam bender, see below), we will be able to place ~1m shielding materials between neighbors[‡], and allow a 2m diameter scattering tube be placed at ~1m after the sample. The use of the beam bender requires that the beam upstream from 10m be enclosed

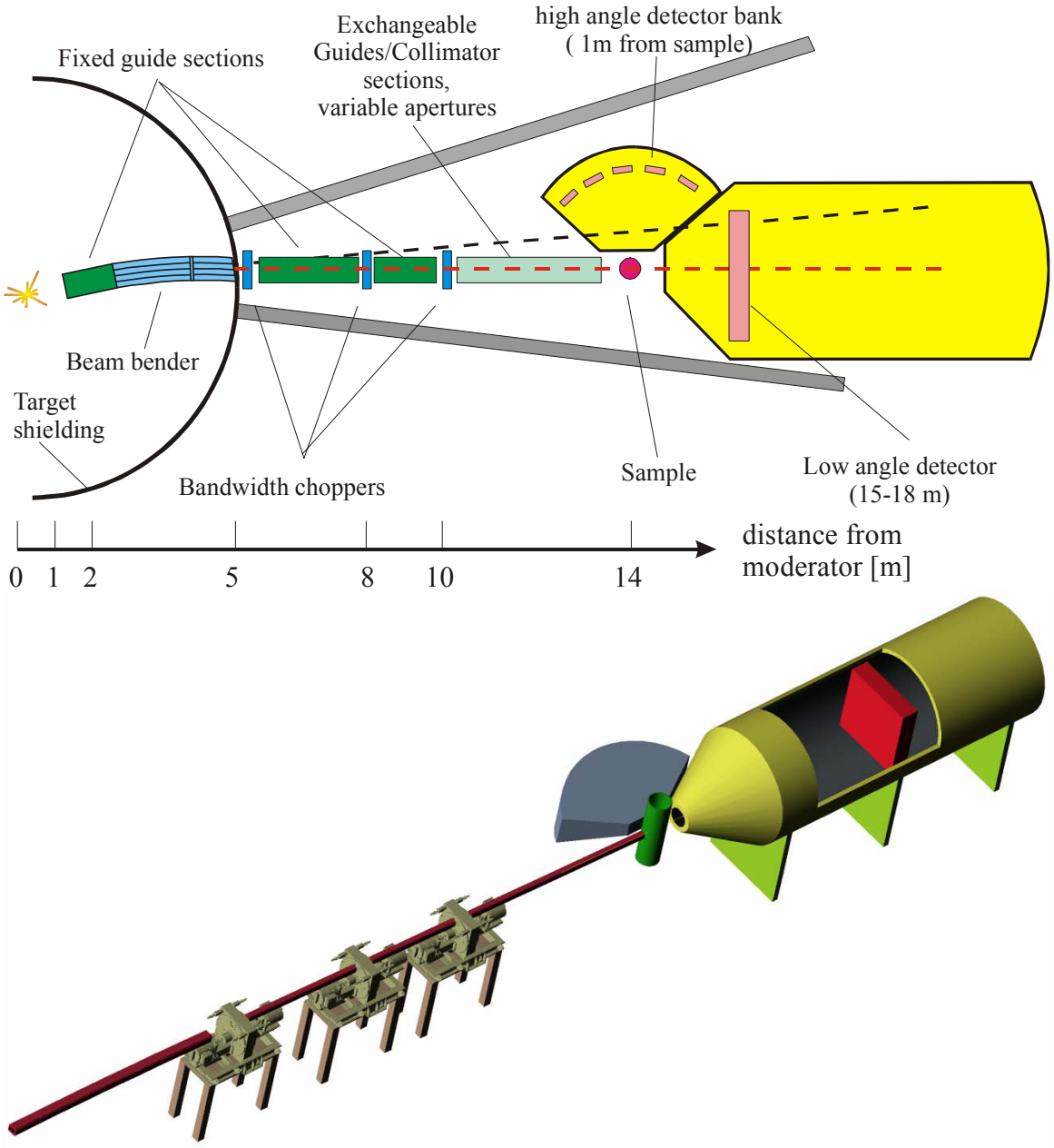

Figure 1. Schematic view (top) and three-dimensional representation (bottom) of the extended-Q SANS.

[†] Unless otherwise noticed, the position parameters in this document are relative to the moderator.

[‡] We contribute 50cm to each side. The shielding requirement between beamlines is currently specified at ~2m, which is thicker than the number we have taken here. However, the next beamline (in counter clockwise direction) is designed for an Engineering Diffractometer, which will be a long instrument and only guides are foreseen at SANS's location. It will therefore provide ~1.5m shielding space in tangential direction at 14m. The beamline on the other side will likely be a long instrument as well. All together, we should have enough space for shielding.

tightly by shielding materials. Moveable guides/collimator sections can therefore only be placed between 10 and 14m. Assuming equal source[§]-to-sample and sample-to-detector distances for a pinhole SANS, the maximum machine length is then given at 18m. By moving the detector closer to the sample, shorter machine lengths (15-18m variable) can be obtained.

Moderator

The Extended-Q SANS will be viewing the top downstream, coupled cold hydrogen moderator on the 60Hz target. At the 18 m detector-to-source distance, the maximum useable bandwidth will be ~ 3.7 Å. The pulse width of the moderator is ~ 18 μs/Å based on neutronics calculations (Iverson/SNS), giving a wavelength resolution of $\delta\lambda/\lambda$ ~0.4%. When the detector is at 15m, the bandwidth and $\delta\lambda/\lambda$ will be 4.4Å and 0.5%, respectively.

Beam Bender System

A crucial component on the Extended-Q SANS is the beam bender system, which consists of a straight guide, a beam bender and a further section of straight guide (Figure 2). The purpose of the bender system is to avoid the direct line-of-sight from the moderator. The design choice is constrained by beam shielding requirements and we have performed extensive Monte-Carlo simulations to optimize the bender system (appendix A, appendix B). The first 1m-long straight guide is located within the target core vessel insert and starts at 1m from the moderator. The curved, 3m-long multi-channel bender is made of two parts. The first 2m is located within the shutter insert while the remaining 1m extends from the shutter to the edge of the target monolith steel. The bender has the bending radius of 65m and is divided into10 bender channels. The straight guide that follows the bender extends from 5m to 10m. The exact locations of these components will be determined at the engineering design stage and we do not expect such slight variations to have noticeable performance impacts. The cross-section of the guides and bender is 4x4cm^2.

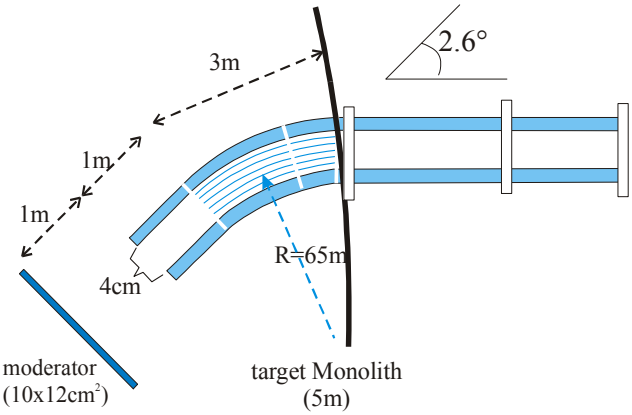

Figure 2 Schematic of the Guide-Bender-Guide system. The three bandwidth choppers at 5, 8, and 10m are indicated as rectangles.

To allow shorter wavelength neutrons to pass through, the bender has to be super-mirror coated. We chose 3.5xNi coating as the baseline design. Better coatings will only enhance the performance. Monte Carlo simulations show that the straight-guide sections will also have to be supermirror coated for maximum performance. Detailed studies supporting the design choices are attached in appendix B.

Choppers

Three standard bandwidth choppers are designed at 5, 8, and 10m. The location of the first chopper is loosely limited between 5 and 5.5m to accommodate possible engineering constraints.

[§] The term 'source' here refers to the source aperture for SANS, which is usually at the end of the guide. This is not to be confused with the source for the whole instrument, which is the moderator.

The edge of the target monolith steel is at ~5m. This three-chopper system will completely eliminate leakage of slow neutrons (Figure 3).

A T0 chopper is not foreseen. A T0 in place of the beam bender will not be enough to block the fast neutrons. The combination of a T0 chopper with the beam bender will cause some ~15% flux loss. A detailed discussion is attached in appendix B.

Moveable Guides and Collimators

The last meter before the sample position (13-14m from the moderator) will have no guides. Between 10-13m from the moderator, there will be three sections of 1m-long, removable guides. The possible collimation lengths on the Extended-Q SANS will therefore be 1, 2, 3, and 4m. These sections will have to be designed to enable tight shielding of the direct beam.

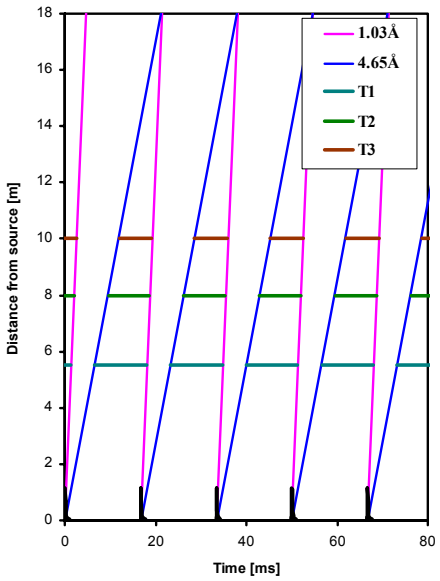

In addition, two 1m-long Soller collimators, one for horizontal and one for vertical collimations, will be provided as a user choice. The purpose of these collimators is to converge the direct beam onto a smaller spot on the detector, thus enabling the access to smaller Q-values. The collimators will be located between 11-12m and 12-13m, respectively. They will be inter-exchangeable with the last two guide sections. The horizontal collimator will have entry and exit channel widths of 0.833 mm and 0.714 mm, respectively. The channel widths for the vertical

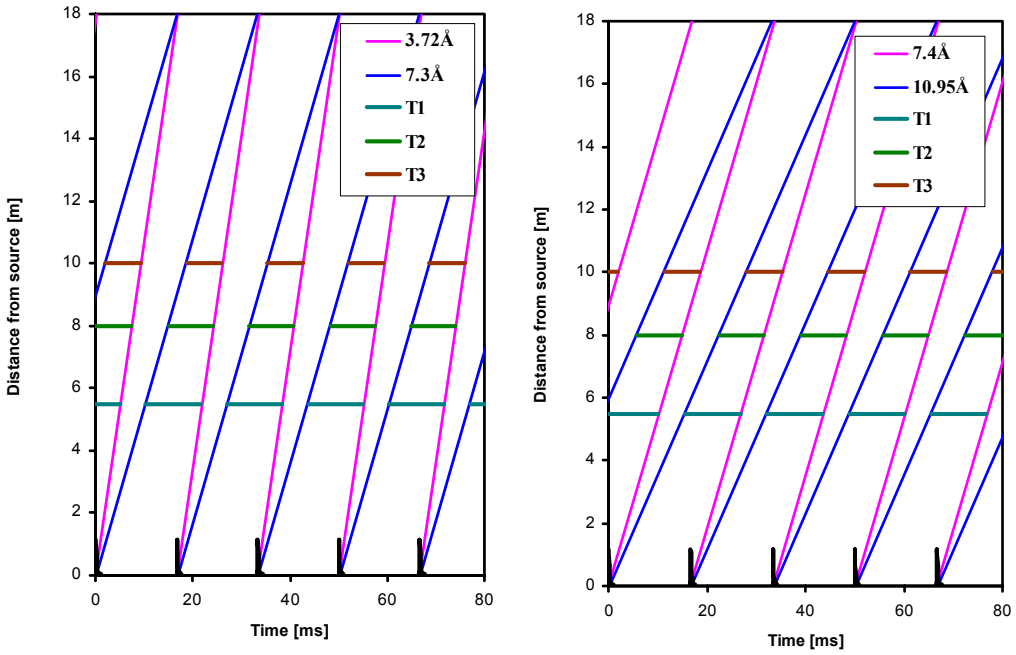

Figure 3. Time diagram of the Extended-Q SANS at the source-to-detector distance of 18-meter. The three figures are for the first, second, and third-frame operations, respectively. The wavelengths shown are those of the umbrae only.

collimator will be 1mm and 0.833mm. The size of the converged direct beam on the detector is 1cm. Detailed discussion on Soller collimator design is attached in appendix C.

Detectors

The main detector will be a large active area (1 x 1 m^2), high counting rate (≥ 10^6 neutrons/sec over the whole detector) ^{3}He detector. The physical resolution of the detector shall be 5mm. Better resolution is desired when Soller collimator geometry is used, especially at very small angle area around the beam stop. Detector maker ORDELA of Oak Ridge has built a smaller version of such a detector (64x64 cm^2), which performs well. ORDELA is currently building a 1x1m^2 detector for the SANS upgrade at HFIR/ORNL. The manufacture's specifications on counting rates are ~ 10^4 n/s per wire and 10^6 n/s on the whole detector. These detectors have a gas pressure of ~ 1.25 bar and a neutron detection efficiency of ~80% at 5Å. The efficiency decreases to ~ 50% for 2 Å neutrons. For use on the Extended-Q SANS, the detector will have to have about twice the gas pressure to have a reasonable counting efficiency for 1-5 Å neutrons. Increasing gas pressure should be a solvable problem by using convex or concave pressure balancing vessels. Higher gas pressure is also desired since it will improve the spatial resolution, which in turn means more detection wires can be used for increased counting rate.

For experiments on the Extended-Q SANS, ORDELA-like detectors will serve most of the needs. For experiments with strong scattering samples, detectors with higher counting rate are desirable (see performance section). There are many competing detector technologies currently in development. Some of these efforts are directed at building large area, high counting rate detectors that will be suitable for SANS applications. We will consider these new detecting technologies as they come along.

The detector will be installed in a 5m-long tube to allow 1- 4 m, variable sample-to-detector distances.

There will be a high-angle detector bank arranged on an arc one-meter away from the sample, covering an angle range of ~35-150°. This bank could for example be made up of standard, ^{3}He area detectors (20x20 cm^2). For diffraction purposes, the detectors could be arranged such that the d-spacing resolution is uniform across all detector pixels. We believe such arrangement will not be necessary for this instrument (for discussion, see appendix D).

To ensure continuous Q-coverage, the minimal number of such detectors is five (Figure 4). Since scattering signals at high angle are often very weak, the high angle detectors will therefore have to cover as much space as possible. Such detectors would therefore be arranged in two rows stacked on top of each other, covering 35-150° in scattering angle and ± 12° off scattering plane. With tight placement, each row could have up to 10 detectors (20x20cm^2), giving a total of 20 high angle detectors.

The SANS user community has also expressed interests in a detector at 180°. This can be achieved by using some of the scintillation detectors currently under R&D, especially those that will allow an opening in the middle for beam feed through.

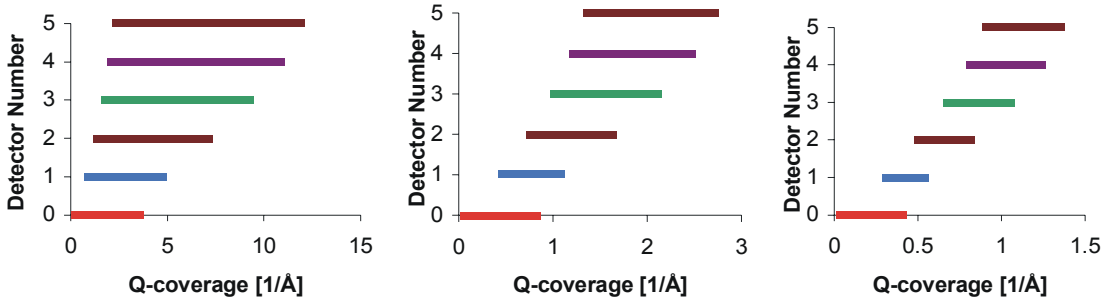

Figure 4. Q-coverage for the Extended-Q SANS to operate in different frames. Only five high angle detectors are shown, which is the minimal number of detectors needed to have a continuous Q-coverage. The additional 15 detectors on the high angle bank overlaps with these five detectors in Q space. Detectors are numbered from 0 to 5 starting from the low angle detector. The low angle detector is positioned at 15m for these calculations. Left: first frame 1 – 5.4 Å, Middle: second frame 4.4 – 8.8Å, Right: third frame 8.8-13.2Å.

User Access and Sample Environment

At 14 meters from the moderator, there will not be enough space for regular user access from the side. Top access will therefore be provided. There will, however, be about ~1m standing space for checking the sample from the side. Various sample environments, such as automated sample exchanger, furnaces, cryostats, and magnets will have to be lowered in place from the top. Precise positioning of these equipments will be provided to ensure the ease of installation and alignment.

Shielding

Beam shielding after the bender, especially immediately around the beam, will be crucial in reducing the prompt spike. The scattering tube will also have to be shielded against the prompt pulse that is not directly coming from the beam channel. Experiences at ISIS at the Rutherford-Appleton Laboratory in England (Heenan, private communication) show that painting the scattering tube on the inside with gadolinium oxide and shielding it on the outside with borated wax is an effective method.

Performance Estimation

Q-range

The minimum accessible Q-value on the Extended-Q SANS is obtained when the low angle detector is at its maximum distance of 18m (4m detector-to-sample). For circular beam geometry with a 1cm sample and 2cm source apertures (source at 10m), a 4cm beamstop will be needed, giving Qmin[**] values of ~ 0.01, 0.006, and 0.004Å^{-1} for instrument operating in the first (~1–4.7 Å), second (~3.7–7.3 Å), and third (~7.3–11Å) frames, respectively. With the use of Soller collimators, the Qmin values for the three frames will be ~ 0.0024, 0.0015, and 0.001Å^{-1}, respectively.

The Qmax value on the Extended-Q SANS will be 12 Å^{-1}, which is given by the use of 1Å neutrons at the highest detector angle of ~150°. Figure 4 shows the Q-coverage of the detectors. The Qmax value on the low angle detector will be 3.5Å^{-1}.

[**] In obtaining Qmin values, we allow ~40% margins from the numbers calculated from geometrical arrangements.

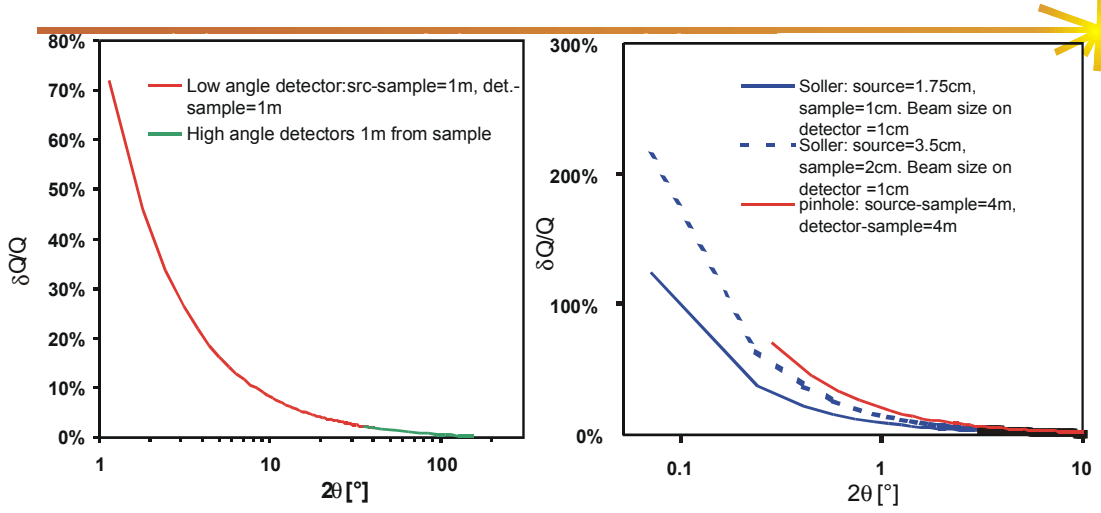

Figure 5. Q-resolution (standard deviation). Left: low-angle detector at 15m. Right: Low angle detector at 18m. Resolutions for Soller collimators with two different sample and source sizes are also shown. Detector pixel resolution of 0.5cm is assumed. The source and sample apertures for pinhole setups are 2 and 1cm, respectively.

The largest *continuous* Q-coverage of 0.01-12Å^{-1} is given by operating in the first frame and the low angle detector is at 18m. If Soller collimators are used, this range becomes ~ 0.0024-12Å^{-1}.

The maximum dynamic Q-range on the low angle detector will be >100. With Soller collimators and including high angle detectors, a dynamic range of close to 5000 can be reached. This value is 100 times larger than that of the current best reactor-based instrument, which is D22 at *Institut Laue Langevin* (ILL) in France.

Resolution

At low scattering angles, the resolution function (δQ/Q) is dominated by geometrical factors. These factors are the sizes and relative positions of the source and sample apertures, and pixel resolution of the detector. In back scattering directions, the geometrical contribution is minimal and the resolution reduces to the level of wavelength spread. δλ/λ (FWHM) determined by the pulse width of the moderator and detector to moderator distances (Figure 5), is 0.5% on the high angle detectors, and 0.4 - 0.5% on the low angle detector.

The use of Soller collimators will improve the resolution for same detector distance (Figure 5). However, the resolution will be worse than pinhole setups with same Qmin-values. The Qmin-equivalent pinhole setup for the designed Soller collimators is when detector-to-sample distance is 16m. Detailed discussions on resolution and resolution for Soller collimators are attached in appendices D and C.

Flux and Count Rate

The fluxes on the Extended-Q SANS are simulated using the Monte-Carlo packages we have developed at SNS (see appendix A). The programs are benchmarked through simulations of the 30m NG3-SANS at the National Institute of Standard and Technology (NIST, see appendix E). The simulated fluxes for the NIST SANS are close to the published numbers (table 1). We therefore believe that the simulated performances for the Extended-Q SANS should be very reliable.

At the end of the fixed guide system at 10m, the time-averaged, per Å flux on the Extended-Q SANS will be comparable to the new SANS at the HFIR upgrade (Figure 6). The performance of the new HFIR SANS is calculated to be similar to D22 at ILL, which is the best SANS machine currently in operation.

When operating in the second frame and with 4m-collimation length, the flux at sample position integrated over the wavelength band (3.66-7.33 Å for detector at 18m) is 2.5 times that of the planned new HFIR SANS operating at $\delta\lambda/\lambda = 10\%$ (Figures 7,8). The gain increases to 7 at 1m-collimation. These ratios reduce to 1.5 and 5 when operating in the third frame (7.33-10.99 Å for detector at 18m).

The detector data rate depends on the sample. Figure 7 shows the simulated available flux at the sample position for different collimation lengths. As a reference, we estimate the maximum per-pixel counting rate in the second frame for an incoherent scatterer (such as water), 1cm^2 in cross-section and 50% in transmission. On a 5mm x 5mm detector pixel, the maximum instantaneous counting rate will be ~650n/s when the detector is at 15m (1m detector-to-sample and 1m collimation). At 4m-collimation and with the detector at 18m, the counting rate will be ~60n/s.

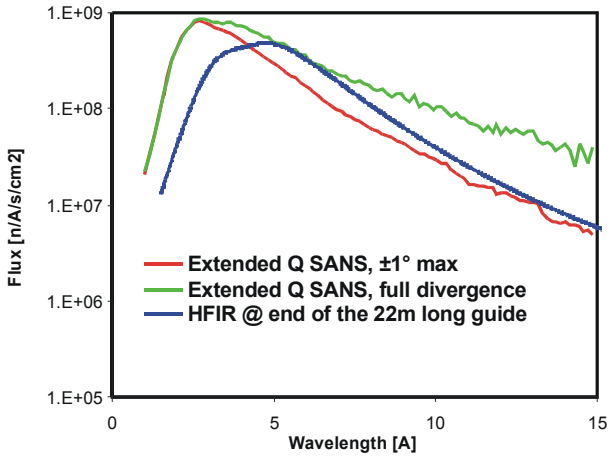

Figure 6. Simulated fluxes after the straight guide at 10m. The down turn bellow ~2.5Å is only partially due to the transmission of the beam bender (compare to appendix A, Figure A1). Replacing the bender with a T0-chopper will improve the flux in this region (appendix B, Figure B5), but will decrease the flux for longer wavelength neutrons (see appendix B, Figures B6&7).
The equivalent location at the planned new SANS at the HFIR upgrade is at the end of a 22m-long straight guide (Ralph Moon/HFIR, private communication).

Data collection time depends both on scattering properties of the sample and on the required Q-range. For strong scatterers, such as polymers at high concentrations, collection of a single data set within one minute will be possible for all accessible Q ranges. For weak scatterers, such as proteins in dilute solutions, the per data set collection time less than 10 min will be possible when Qmin~0.001 Å is needed. For Qmin~0.006 Å, collection of a single data set with sufficient statistics will be possible within 1 min.

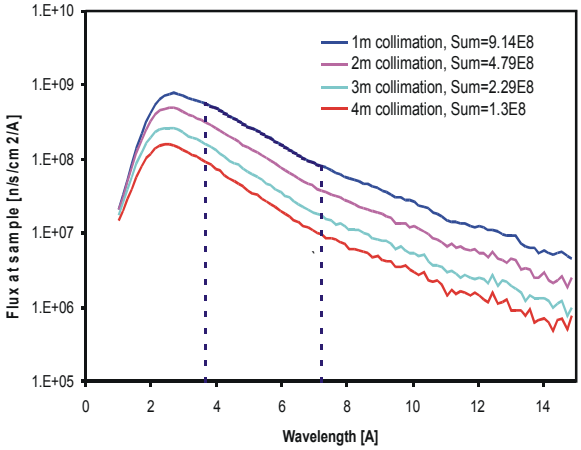

Figure 7. Simulated, time averaged flux at sample position. The region between the dotted lines corresponds to the second frame when detector is at 18m. The *'sums'* in the legend are the integrated flux within the second frame.

The best SANS currently operating in the US are the two 30m SANS machines at NIST. The Q-range on the NIST-SANS is 0.0015-0.6Å^{-1}(Glinka et al. *J Appl. Cryst.* 1998 31,430-445, "*The 30m SANS at NIST*"). Table 2 and Figure 9 compare total fluxes on sample vs. accessible Q-Range for the Extended-Q SANS

with the NIST SANS. When accessing same Qmin values, the integrated flux at sample position on the Extended-Q SANS will be ~ 20x that of the 30m SANS at NIST. An interesting configuration on the Extended-Q SANS is when operating in the second frame and the detector is at 18m (4m sample-to-detector). The Q-coverage on the low angle detector will be 0.006 - 0.25 $Å^{-1}$(table 1), which is suited for studying most proteins and small to mid sized protein complexes. On reactor-based SANS instruments, two or more instrument configurations will be needed to cover the same Q-range. Since biological samples frequently have time-dependent properties, experimentally desired (e.g. kinetics) or undesired (e.g. aggregation), the ability to simultaneously collect data over all the required Q-range is often a prerequisite to study these systems.

Further R&D

We have an ongoing effort to study focusing optics. One of the promising techniques is the use of multi-channel focusing guides in combination with Soller collimators. Such optics should increase the performance of this instrument.

Detector R&D will be very important to this instrument. ^{3}He based gas detectors are at their limits, especially in counting rate. We are very hopeful that large active area, high counting rate, and high resolution scintillation detectors will be available soon.

Better understanding of the background will also be

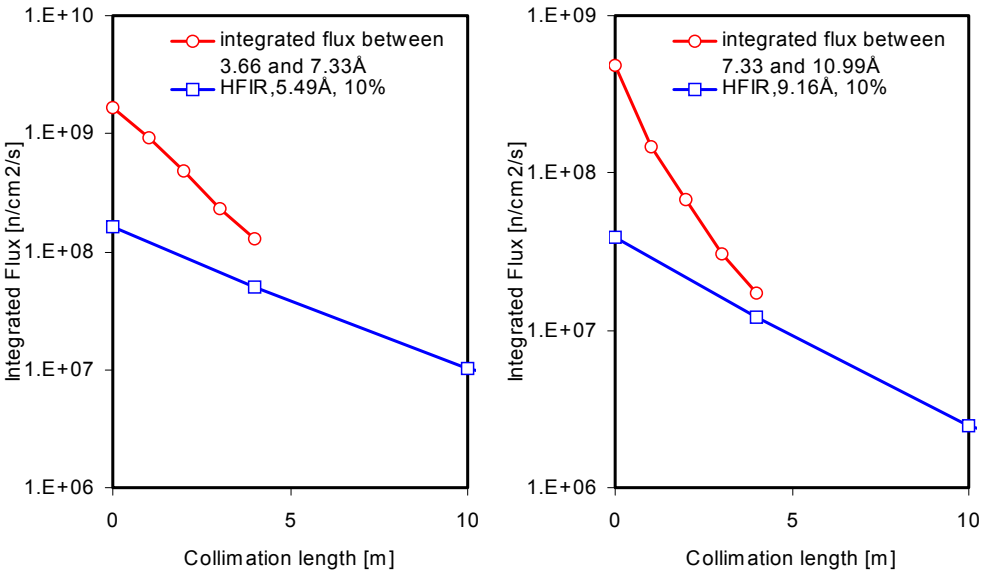

Figure 8 Integrated flux at sample position vs. collimation length in the first (top), second (bottom-left) and third (bottom-right) frames. The detector was positioned at 18m for these calculations. Flux integration for planned new SANS at HFIR upgrade (Ralph Moon/HFIR, private communication) is taken in the middle of each frame with 10% δλ/λ FWHM. The flux ratios to HFIR-SANS in the second frame are 2.5 and 7 at 4 and 1m collimations, respectively. In the third frame, these ratios are 1.5 and 5.

Note that the new HFIR SANS is not designed to operate in the wavelength range of the first frame. The first frame figure is therefore for reference only.

required to effectively shield the detectors and thus increase the signal-to-noise ratio. At the location of the Extended-Q SANS, we believe that there will be enough shielding space to prevent cross-talks between beam lines. The unknown source of background is therefore primarily from the beam channel. One of the concerns is that the beam bender system on this instrument may act as a moderator, or secondary source. Fast neutrons from the prompt pulse will be scattered and slowed down by the bender, which may in turn have noticeable effects in instrument backgrounds. MCNP simulations will thus be needed to study how severe such effects will be. The results will aid us in choosing proper shielding strategies, such as the use of T0 choppers in combination with the bender.

Possible backgrounds caused by surface scattering from the Soller collimators will also need to be studied.

Conclusion

The Extended-Q SANS on the 60 Hz target will be a unique instrument. Its wide Q coverage and high wavelength resolution are unmatched by any existing SANS instruments. The minimum accessible Q-values will be very competitive, especially when Soller collimators are used. It will have the highest useable flux at the sample position. Depending on Q-ranges, the flux on sample will be at least one order of magnitude higher than the current best SANS instruments in the U.S.

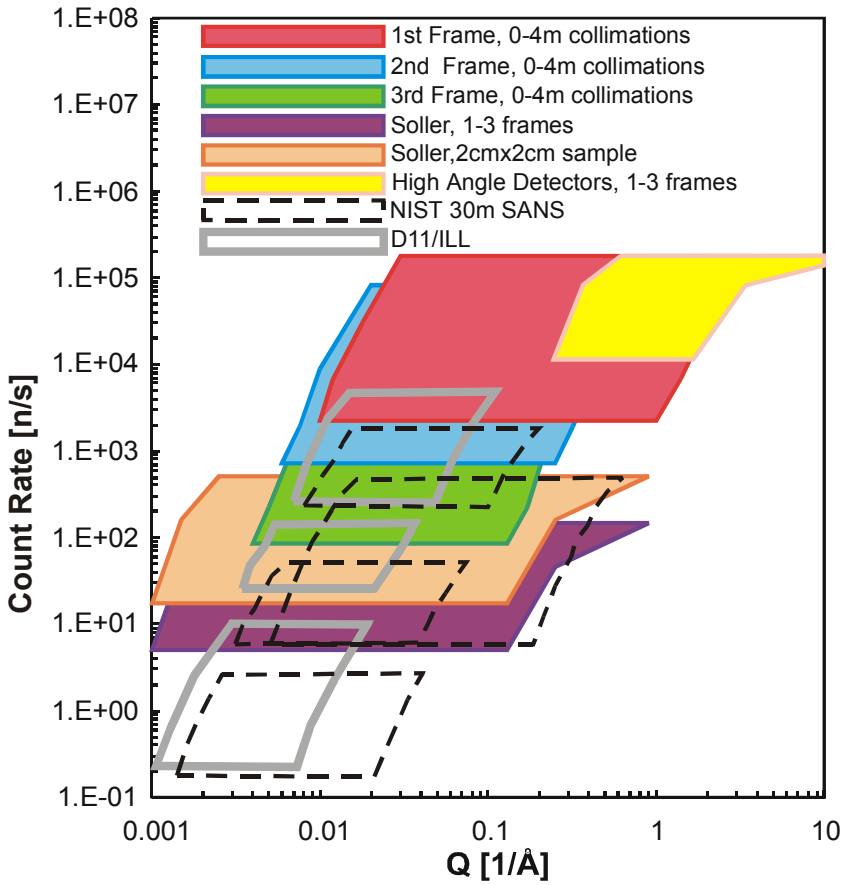

Figure 9 Simulated count rate vs. accessible Q-range. The rate is calculated, as in "Glinka et. al., J. Appl. Cryst. 1998, vol 31, 430-445", by multiplying flux on sample with sample area and the solid angle of a detector pixel. The sample area for all calculations is assumed to be 1cm^2. The detector pixels for the extend-Q SANS is scaled to 1 cm x 1cm to match the condition with the NIST SANS. The D11/ILL data was adapted in Glinka et al from Lindner et al, Physica B, vol 180-181,967-972.

Table 1. Integrated Flux on Sample vs. Qmin

Extend-Q SANS						30-Meter SANS, NIST (δλ/λ =15%, reactor at 20MW)				
			Simulation conditions					Integrated flux (over sample area)		
Qmin-Qmax[(q)] [Å^{-1}]	Qmax/Qmin	Simulated, integrated flux on sample [10^6 s^{-1}]	Sample aperture diameter [cm]	Detector to sample [m]	Frame No	Qmin-Qmax [Å^{-1}]	Qmax/Qmin	Measured[($)] JAC[(J)] [$10^6$ s^{-1}]	Measured[($)] Web[(w)] [$10^6$ s^{-1}]	Simulated[(#)] [10^6 s^{-1}]
0.001-0.15[(s)]	150	0.8, 3 [(2cm)]	1	4	3					
0.0015-0.3[(s)]	200	7, 25[(2cm)]	1	4	2	0.0015-0.013[(10Å)]	9	0.09	0.1	0.16
0.004-0.13	33	14	1	4	3	0.002-0.019[(7.5)]	10	0.26	0.3	0.48
0.006-0.25	42	120	1	4	2	0.003-0.025	8	0.85	0.86	1.7
0.008-0.35	44	170	1	3	2	0.0064-0.04	6	6.38	5.65	12.5
0.01-0.5	50	360	1	2	2	0.016-0.1	6	30.9	-	68
0.02-0.8	40	820	1	1	2					

[(q)] The Qmax values are from the low-angle detector only.
[(s)] with Soller collimators.
[(2cm)] with 2cm diameter sample. The fluxes are integrated over the whole sample area.
[($)] integrated over sample apertures, which are 1.9cm for Qmin<=0.003 and 2.5cm for Qmin>=0.0064.
[(J)] values from Glinka et. al. (J. Appl. Cryst. 1998, vol 31, 430-445).
[(W)] values calculated from using calculation tools on http://www.ncnr.nist.gov/.
[(#)] simulations were performed for the SANS on NG3. For details, see appendix E.

Table 2. Extended-Q SANS parameters

Moderator:	
Rep rate	60 Hz
Power	2 MW
Location	Top down stream
Type	Coupled LH2, Be reflector
Pulse width	~ 18 μs FWHM per Å
Choppers	All choppers are from standard SNS design
T1	5 m
T2	8 m
T3	10 m
Beam bender	
Location	2-4m, 4-5m
Total Length	3 m
Cross-section	4x4 cm^2
Number of Channels	10
Coating	3.5× Ni-θc super mirror
Total Bending angle	2.6 °
Neutron Guides	
Location	1-2m, 5-10m (fixed) 10-11m, 11-12m, 12-13m (removable)
Coating	3.5× Ni-θc super mirror

Collimation and apertures	collimation: 1,2,3,4 m variable sample aperture: 1-2cm source aperture: 2-4cm Optional Soller collimators	
Beam Tubes	Evacuated (≤ 0.01 mbar) rectangular tube with inner cadmium or gadolinium coating. The two horizontal tube walls have to be part of the shielding.	
Sample environment Location Maximum ancillary equipment size Sample Size	Open area to accommodate ancillary equipments. 14 m ~1m in diameter ≤ 2 cm for pinhole setup ≤2.3cm with Soller Collimators	
Low-Angle Detector Size Pixel resolution Beam stop Location	^{3}He gas technology. 1 x 1 m^2 5 mm 4x4 cm^2, 1x1 cm^2 with Soller collimators. 15 – 18 m, continues	
High-Angle Detector Bank Location Number of detectors Detector Size Pixel resolution Total Angle coverage	^{3}He gas technology. 1m from sample. 20 20 x 20 cm^2 5 mm 35° - 150°	
Scattering chamber	Evacuated (0.01 mbar), 2m diameter cylinder, with gadolinium oxide painting on the inside and borated wax on the outside. Automated detector rail mounted inside.	
Data Acquisition	Standard system with online data reduction.	
Q –range Q-min Q-max	 0.004 Å^{-1} with pinhole geometry 0.001 Å^{-1} with Soller collimators 3.5 Å^{-1} on low angle detector 12Å^{-1} on high angle detector	
Resolution	Low-angle detector	High-angle detectors.
δλ/λ (FWHM) δQ/Q (FWHM)	0.4-0.5% > 5%	0.5% <5% (≤ 1% for back scattering)
Flux and counting rate Maximum per 5x5mm^2 pixel count rate	650n/s (with incoherent scatterer)	

Appendix A Monte Carlo Simulations

Simulation Tools and Benchmarking

A Monte Carlo package developed by the author was used to simulate the Extended-Q SANS and its components. The simulation tools are benchmarked through simulating the NIST 30m SANS on NG3 (appendix E). The simulated fluxes are within a factor of ~2 of published data. We have consulted many Monte-Carlo experts and the consensus is that the factor 2 is warranted considering the NIST 30m SANS has more than 40 meters of neutron guides. Simulations referred in this document do not take into account the surface roughness and flatness of the guides, nor do they consider the accuracy of guide alignment. Many other factors, including window materials in neutron flight path, all degrade the actual performance of an instrument, but are not simulated here. From the benchmarking result, the estimated performance for the Extended-Q SANS should be accurate within factor 2. We did not attempt to correct the performance estimates on the Extended-Q SANS by this factor for three reasons. First, the major performance comparison for the Extended-Q SANS is with the new SANS at HFIR upgrade, which will be a D22/ ILL-type instrument. The performances for the HFIR SANS are simulated as well. Second, as will be discussed bellow in the *source* section, it is highly likely that the upper down stream moderator will be optimized to give 2x more flux. Third, for the Extended-Q SANS, the accumulated effects from all the factors that affect the actual instrument performance should be smaller than for the NIST 30m SANS, since it has only 14m primary flight path, whereas the NIST 30m SANS has ~49m (appendix E). The deviation between the actual and simulated performances on the Extended-Q SANS will therefore most likely be smaller than the factor 2.

Simulation Conditions

Unless otherwise specified, all simulations in this document assume the following conditions:

Source

Simulated source spectrum for the top down stream, coupled cold moderator was used (Iverson/SNS, Figure A1). The time-averaged flux between 3.7-11 Å (second and third frames on the Extended-Q SANS) is ~13.6% that of the horizontal cold source at ILL (Figure A1). Therefore, in the current configuration, the coupled, cold moderator on the 2MW SNS target is equivalent to an 8MW steady state source. Moderator optimizations are currently underway, which should result in twice or more available flux. These optimizations include tighter coupling, and moving the moderator further upstream to a closer distance to the moderator.

The maximum source divergence used was 1° (except for Figure 6). This value was chosen because it is close to the maximum useable divergence for typical experiments on the Extended-Q SANS. Assuming the use of 1cm sample, 2cm source apertures and a minimum collimation length of 1m, the maximum useable divergence will be ~0.86°. Notice that this value is not the limit on neutron divergence at the sample position. With neutron guide starts at 1m from the moderator (appendix B), the maximum acceptable divergence for the designed neutron optics is ~4.5°. For 1-13 Å neutrons, the divergence values are therefore limited by the guide and mirror coatings to 0.35°/Å. Beyond 13 Å, all neutrons accepted by the guide system can be transported.

Guides and Bender

Coatings for the bender and guides were assumed to have 80% reflectivity and critical angles 3.5 time that of natural nickel (3.5x Ni, or 0.35°/Å). Neutron reflectivity was assumed to be 1 if the incident angle is ≤ 0.1°/Å, and linearly decrease to 80% if the angle is between 0.1 - 0.35°/Å. For incident angled beyond 0.35°/Å, the reflectivity was assumed to be 0.

The substrate for the inner bender channels was assumed to be transparent. The implication of this assumption for the simulation is that neutrons with incident angles < 0.35°/Å but not reflected due to the 80% reflectivity will have a second chance to be reflected by the next channel. Depending on the number of channels the bender has, there will be ~3 - 5% flux penalty if opaque substrate is assumed.

Flux vs. Collimation

The simulation for flux vs. collimation assumed a 4cm x 4cm source slit at the end of the guide and a 2cm x 2cm slit at the sample position. This configuration was chosen to match the conditions for HFIR simulations.

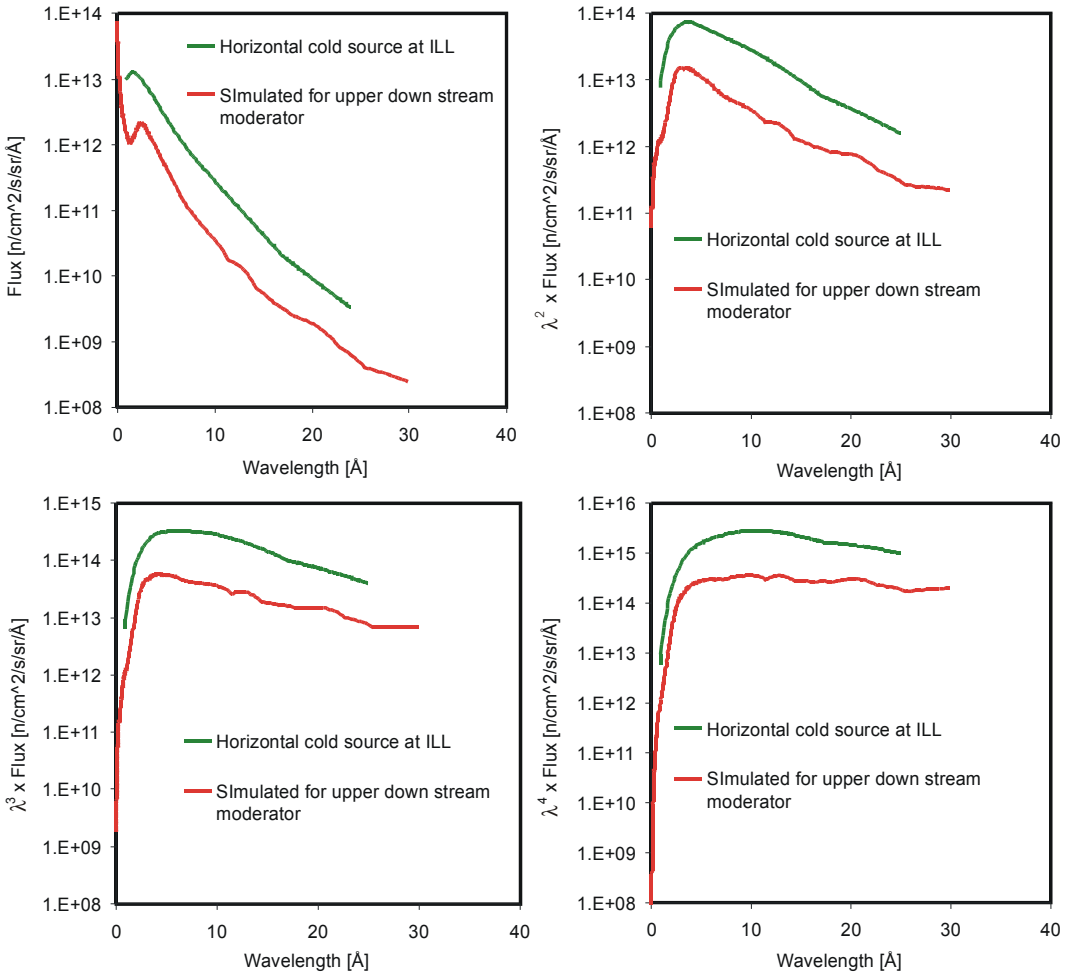

Figure A1 Simulated, time-averaged moderator brilliance for the top-down stream moderator (Iverson/SNS). For comparison, the horizontal cold source at ILL (Ageron, NIM A284,1989,197-199) is also shown. Depending on the problem of interest, the scattering power of neutrons can be scaled with wavelength of different orders. Such scaling ranges from λ^2 (Guinier region) to λ^4 (Porod region). Spectra with three different weighting factors are shown. For small angle scattering, the more relevant scaling should be the use of the Guinier region, i.e. λ^2. In this region, access of same minimal Q-values with shorter λ requires longer collimation length that is inversely proportionally to λ. The flux at sample position is approximately proportional to the inverse of collimation length squared. For other regions and when shorter wavelength is used, data can always be collected at smaller angles to access the same Q-region, without the need of changing collimation length.

Appendix B The Bender System

For the short, 18m SANS instrument, the beam bender should start as early as possible to achieve sufficient beam bending. The closest such place at SNS is ~1m from the moderator within the core vessel insert. At this short distance, radiation and heat damages on the supermirrors could be a concern. Even though experiences at Paul-Scherrer Institute in Switzerland indicate that the supermirrors will most likely be able to endure the strains, we decide to start the beam bender at a safer location of two meters from the moderator, i.e. within the beam shutter.

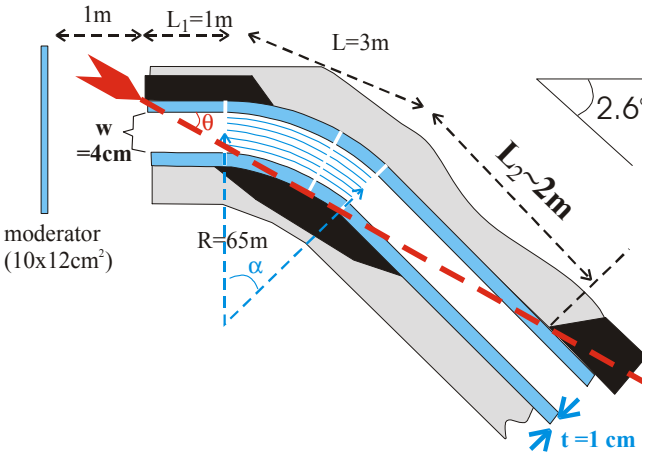

Figure B1 Schematic view of the guide-bender-guide optical system. The system will have to be tightly enclosed by shielding materials (gray shaded area). Locations where shielding is especially important are shaded in black. L_2 is the distance after the bender, at which total blockage of the direct view from the moderator starts. L_2 is determined using the geometrical relations (for the red line):

$$L_2 = xL_1 + R_2 \tan(\frac{\alpha}{2})(x-1) \quad \text{with } \alpha = \frac{L}{R};\ x = \frac{\sin(\theta)}{\sin(\alpha-\theta)};$$

$$\theta = a\cos(\frac{R_1}{\sqrt{(R_2^2+L_1^2}}) - a\tan(\frac{L_1}{R_2});\ R_1 = R - \frac{w}{2} - t;\ \text{and } R_2 = R + \frac{w}{2} + t$$

The chosen bender system is the well-established guide-bender-guide design. The first straight guide section is one meter long and will be located at 1-2m. The curved, multi-channel bender is located between 2-5m, two third of which is inside the main beam shutter (2-4m) and the remaining one third is located between the beam shutter and the edge of the target monolith steel. A further section of straight guide follows the multi-channel bender (Figure B1).

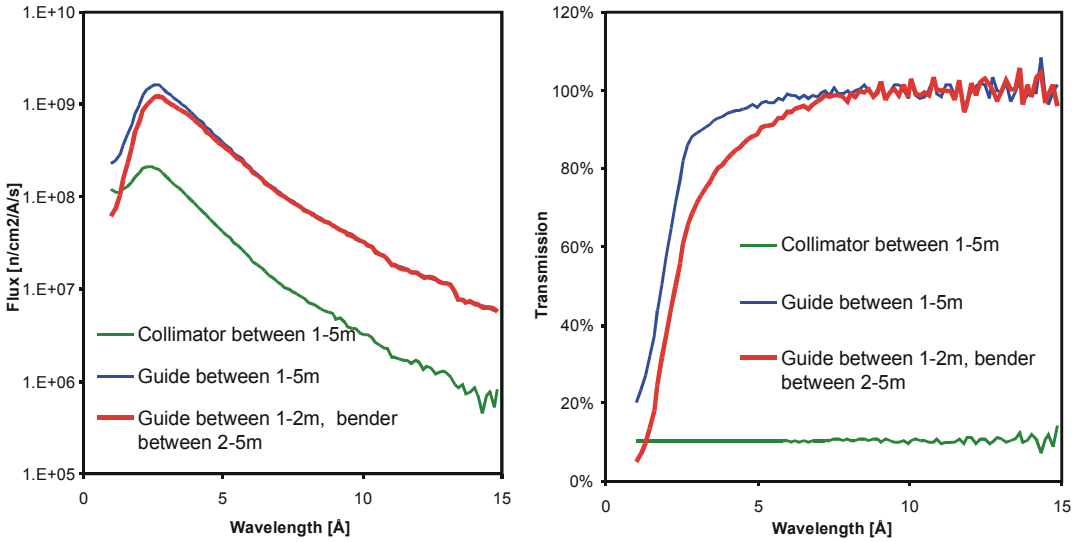

Figure B2. Left: Simulated fluxes at the exit end of the 10-channel, R=65m bender with 1° max source divergence. For comparison, the performances of a straight guide and a collimator are also shown.
Right: Transmissions, as obtained by comparing to the flux at 1m from the moderator.

Bending Radius

The bending radius was chosen to be 65m using the following criteria: at the position of the last chopper at 10m, where moveable parts of the neutron optics start, there have to be at least 2m of shielding materials blocking the direct view from the moderator[††]. For the 4cm wide neutron beam and assuming 1cm thick guide walls, total blockage of the direct beam will start 2m after the bender at ~7m (Figure B1). This will give ~3m of shielding space before 10m. The extra 1m over the above-mentioned criteria is to account for the gaps created by the bandwidth choppers at 8m and 10m (Figure 1).

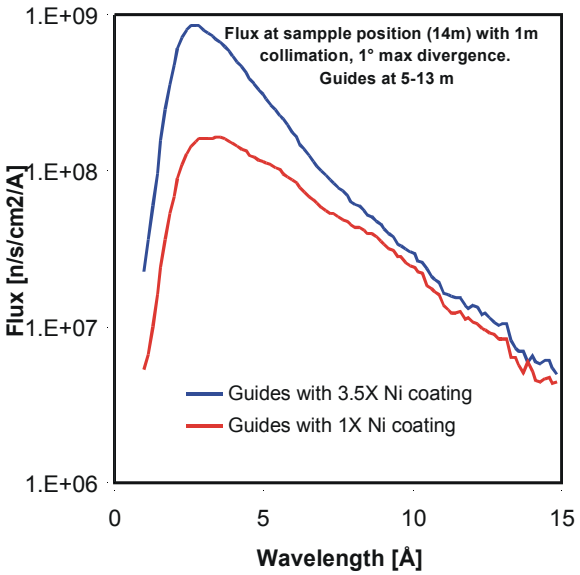

Figure B3 Fluxes at the sample position (14m) with 1m collimation and 1° max source divergence. The coatings for the bender and the guide at 1-2m were kept at 3.5 x Ni. Only coatings for all the guides after bender (8m total) varied.

Number of Bender Channels

With the 3.5X-Ni coatings, the number of channels for the bender is optimized to be 10 through Monte-Carlo simulations. The neutron transport property of the bender is shown in Figure B2.

For maximum performance, the straight guides before and after the bender will also have to be super-mirror coated. Figure B3 shows the flux comparison at sample position with 3.5X and 1X-Ni coatings. Clearly, there is a big flux loss with 1x-Ni coatings.

To simulate the condition if the straight guide between 1-2m is lost to radiation or heat damages, calculations with this guide section replaced with a collimator were performed (Figure B4). Depending on neutron wavelength, the flux losses are up to 35%. Such losses are far less critical than if the bender is placed at 1m and damaged.

[††] Note that there is an additional distance of 4m between the last chopper at 10m and the sample at 14m. About ~3m of this space can be filled with shielding materials. The total shielding between the moderator and the sample will thus be ~ 5m.

Alternative Bending Radii

Engineering constraints on shielding may require more beam bending. We have therefore considered other bending radii as backups. Figure B5 shows the flux ratio at the end of a 12-channel bender with 50m bending radius as compared with the bender chosen for the Extended-Q SANS. The 50m bending radius would give ~4m total shielding space between the bender and the last chopper at 10m. Even though there is a clear flux penalty at shorter wavelength, such bender could be used as an alternative if it is absolutely needed.

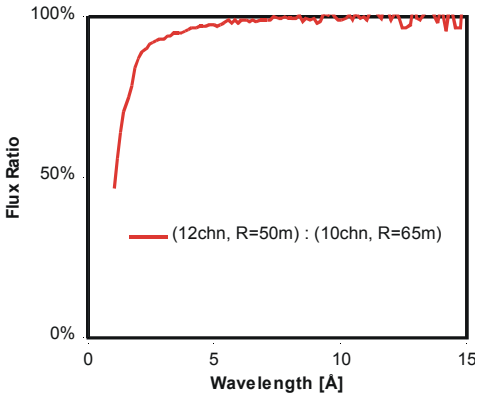

Figure B5. Ratio of simulated fluxes at the end of two benders with different bending radii and channels.

T0 Chopper as Alternative or in Addition to the Beam Bender

Replacing the bender with a straight guide increases the transmission for short wavelength neutrons (Figure B6). Without the bender, a T0 chopper will then have to be used to block the prompt pulse. The gap associated with the T0 chopper will cause ~ 15% loss in flux (Figures B6, B7). For experiments that use the second and third frames (>3.7 Å), the beam bender will therefore deliver a better performance in term of neutron flux. For operating in the first frame, it is not clear how much the gained flux can translate into gains in signal-to-noise ratio, because the 30cm thick T0 chopper, as is currently designed, will not be enough to block the prompt pulse and thus the background will be worse.

Further R&D will have to be conducted to evaluate the performance of the bender-T0 chopper combination in terms of background reduction. The likely scenario that will need such a design is that the materials making up the bender will act as moderators for the fast neutrons, and these

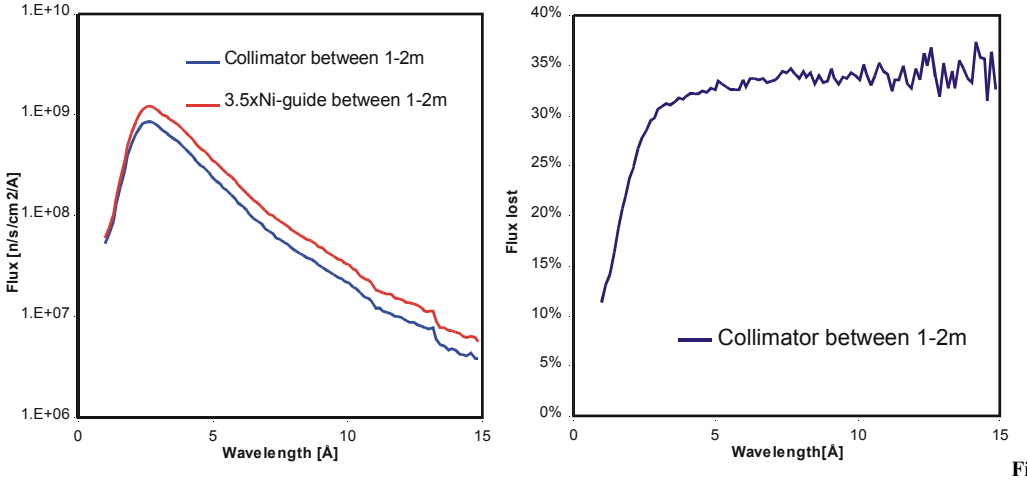

Figure B4. Left: Neutron flux at the end of the bender with 1° max source divergence. Right: Flux loss when the guide between 1-2m is replaced with a collimator.

secondary sources may have noticeable contributions to the background. At this stage, such

combination does not seem to be necessary. The flux loss caused by the T0 chopper is also not desired. (Figure B7).

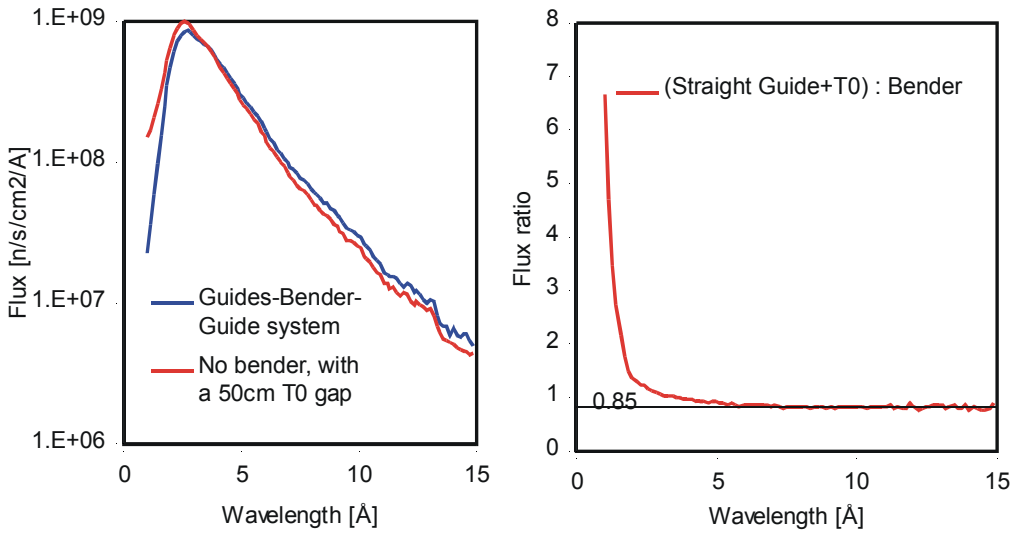

Figure B6 Left: Flux at sample position (14m) with 1m collimation and 1°maximum source divergence. In the case of T0 chopper, the bender is replaced with a straight guide of same coating. A 50cm wide gap is used to represent the condition of a 30cm T0 chopper. Right: Flux ratio between using T0 chopper and using the bender.

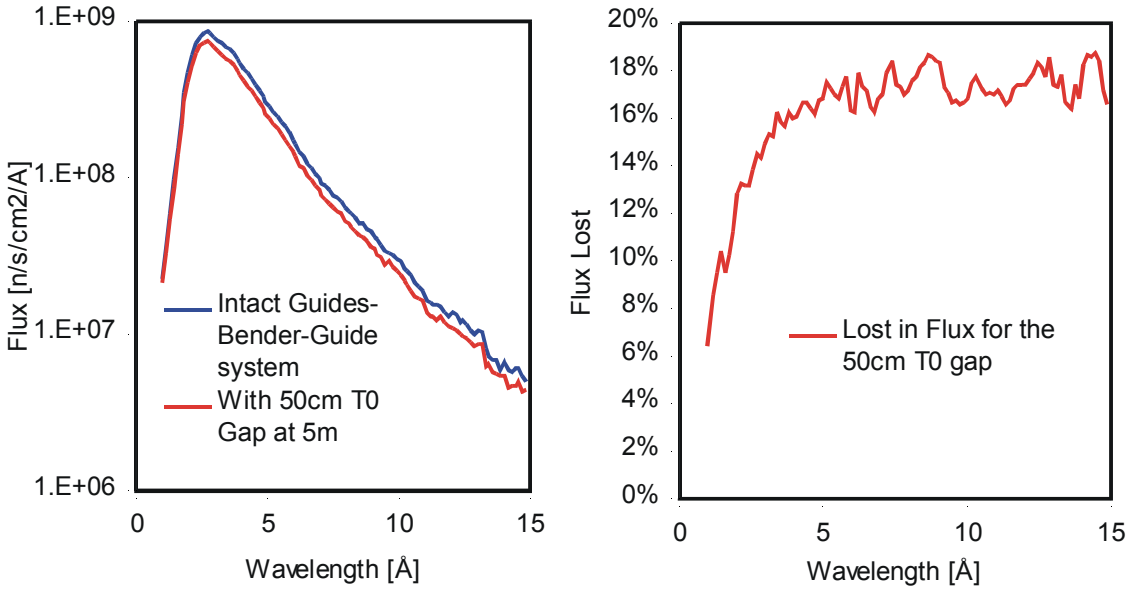

Figure B7 Left: Flux comparison at sample position (14m) with 1m collimation and 1° maximum source divergence. A 50cm wide gap in the guide system is used to represent a T0 chopper.
Right: Loss in flux caused by a T0 chopper.

Appendix C Soller Collimator

Typical experiments on the Extended-Q SANS will have a sample size of~ 1cm. For an optimal pinhole setup, we will need a 2cm source aperture at the end of the guide and equal sample-to-source and detector-to sample-distances. The direct beam spot size on the detector will then be ~ 4cm. The minimum accessible Q value is thus limited by the size of the beam stop and the maximum sample-to-detector distance. With the maximum machine length of 18m on the Extended Q-SANS (4m sample-to-detector), the only way to access smaller Q values is to reduce the size of the direct beam on the detector. Soller collimators provide a nice and simple way to achieve such goal (Crawford&Thiagarajan *Advanced Neutron Sources*,1988).

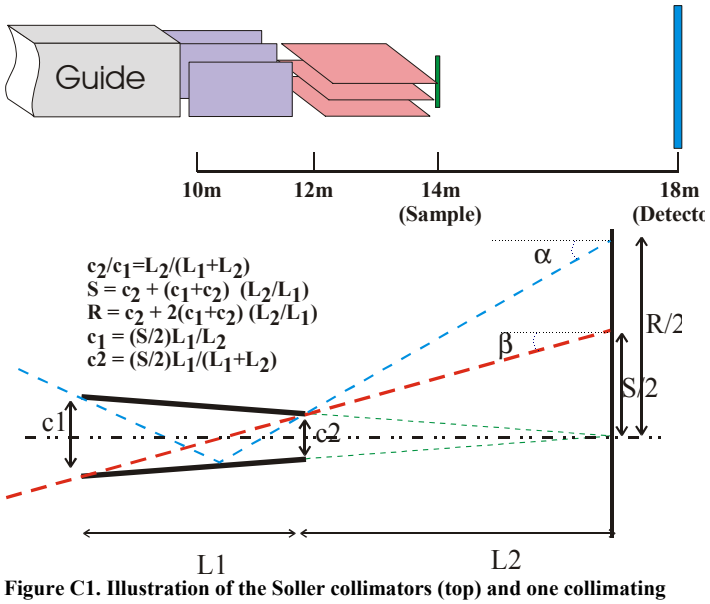

Figure C1. Illustration of the Soller collimators (top) and one collimating channel focusing onto the detector. The beam size on the detector due to first order reflections would be ~ twice that of the direct beam.

Design parameters

Cross-Soller designs will be used for the Extended-Q SANS. Both the horizontal and vertical Soller collimators will be 1m long. They will be located at 11-12m and 12-13m, respectively. To have a 1cm direct beam on the detector (at 18m), the required channel widths are 0.833mm and 0.714mm for the horizontal, and 1mm and 0.833 mm for the vertical collimators, respectively. The dimensions of a single channel determine the size of the direct beam on the detector (Figures C1, C2). The size of the sample aperture has no effect. In principle, these collimator channels could be made very small to achieve small direct beam size. However, because the low-angle

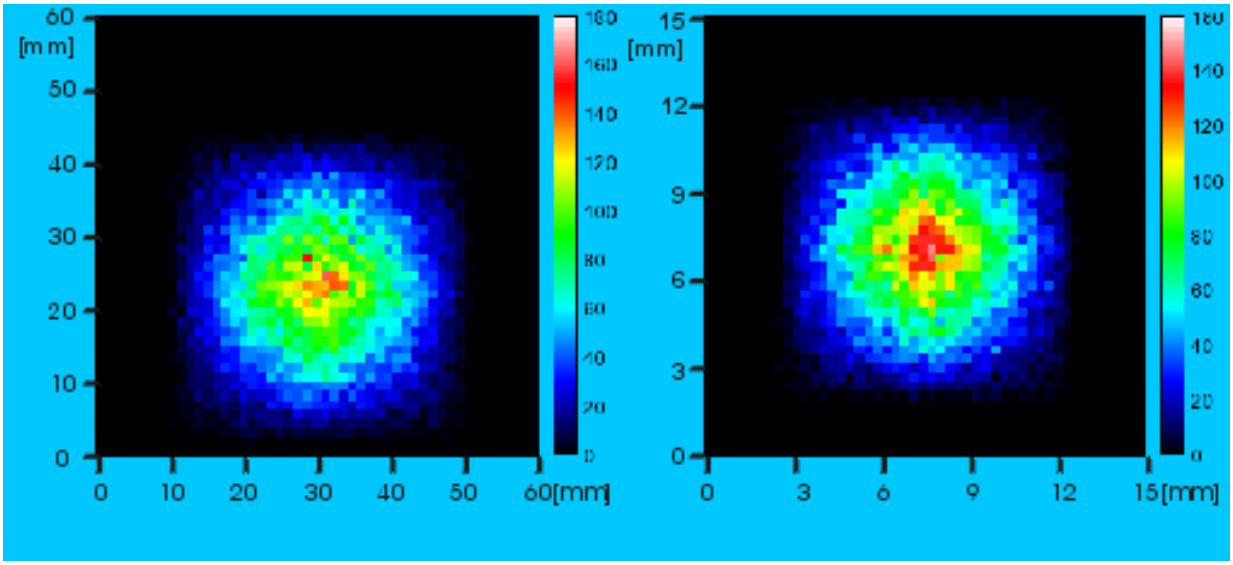

Figure C2. Simulated direct beam on the detector with pinhole setup (left) and Soller collimators (right). For the pinhole setup, sample-to-source and detector-to-sample distances are both 16m. The source and sample apertures are 2 and 1cm, respectively. The Soller collimators converge on the detector plane 4m from the sample with designed 'focusing' spot of 1cm. Simulations were performed for 10 Å neutrons. The downward shift of the direct beam with respect to the detector center corresponds to the freefall of the neutrons between sample and the detector.

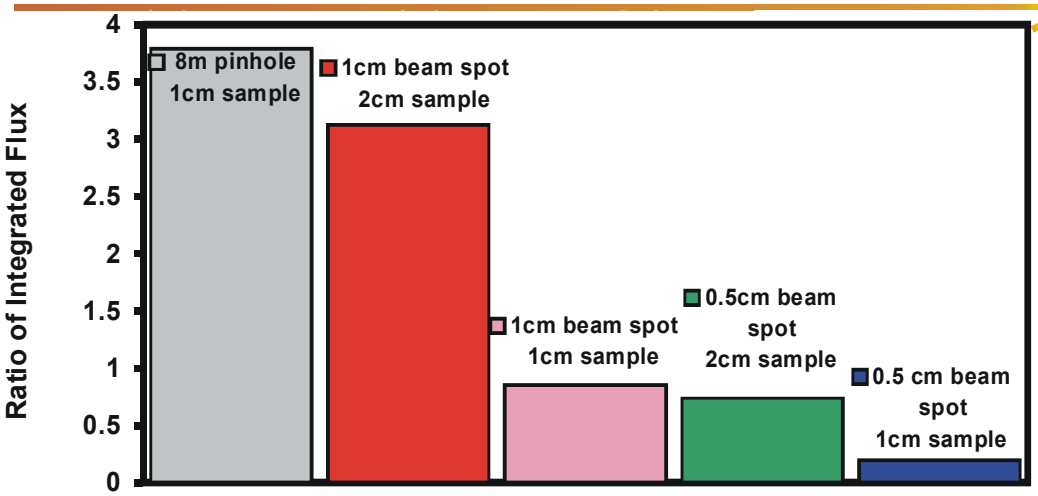

Figure C3 Simulated, integrated fluxes at sample position, shown as ratios to a 16m pinhole geometry (sample-to-detector =detector-to-sample =16m). The source sizes in the Figure legend are the aperture sizes at the entrance of the Soller collimator at 11m. The sample apertures for the 16m and 8m pinholes are 1cm.
The 8m-pinhole has the same resolution to Soller collimators with 1cm sample aperture (Figure C4).

detector for the Extended-Q SANS has a finite resolution of 0.5cm, the practical minimal beam size on the detector is limited to ~0.5-1cm.

Minimal Accessible Q-Value and Total Flux

For a 1cm beam spot size on the detector, the minimal accessible Q-value on the Extended-Q SANS will be equivalent to a pinhole set up with a 16m sample-to-detector distance and a 4cm beam stop. The simulated flux at sample position for both setups is very close to each other (Figure C3). Because the sample size has no effect on the accessible Qmin, larger samples can be used to increase the total data rate in the case of Soller collimators. When using the Soller collimators, one section of 1m-long movable guide can be used at 10-11m. With the designed guide cross-section of 4x4cm^2, the practical limit on sample size is given at ~2.3 x 2.3cm^2.

Resolution

The tradeoff for the gained Qmin and total flux on sample with Soller collimators is resolution (Figure C4).

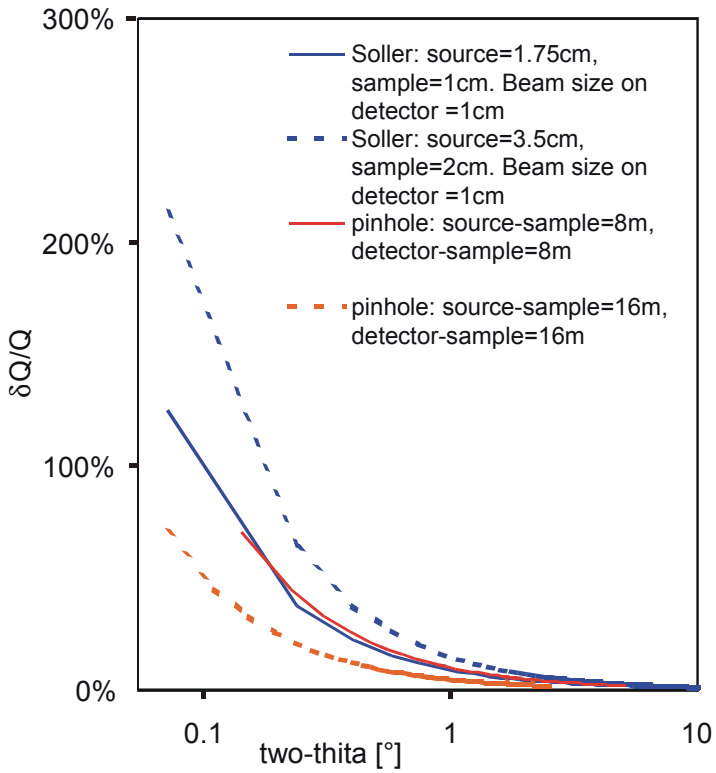

Figure C4 Resolution functions with Soller collimators. Two pinhole setups are also shown. The source sizes in the figure legend are the aperture sizes at the entrance of the Soller collimator at 11m. The sample apertures for the pinhole setups are 1cm and the source apertures for all setups are twice their respective sample apertures. The projections of the curves on the two-theta axis correspond to the angular coverage for each setup. The values are calculated using equations derived in appendix D.

When accessing equal Qmin values, δQ/Q for Soller collimators is ~2x that of a 16m pinhole setup (Figure C4). Comparing to a pinhole-setup with the same sample-to-detector distance, however, the δQ/Q values for Soller collimators is only half as high (Figure 5 in main text).

Comparing to sample and source apertures, the contribution to the resolution function by the sizes of each collimating channel is negligible to the first order. Since the dimensions of the collimating channels determine the beam spot size on the detector, the Q-resolution has therefore no correlation with the size of the beam spot.

Reflections and Scatterings

Reflections from the collimator channels are possible, even though they should be very weak (Crawford & Thiagarajan *Advanced Neutron Sources*,1988). The first order reflections have twice the spot size on the detector than the direct beam (Figure C1). Therefore, if the collimators are designed to converge onto a 0.5 cm beam spot and a 1cm beamstop is used, the background due to the reflections should be eliminated. Smaller beam spot size requires smaller collimating channels, which may make the collimators difficult to manufacture. Experiences at IPNS (Thiagarajan & Crawford, private communication) show that the reflection can be greatly reduced by increasing the surface roughness of the channels. Another source of background is surface scattering from the collimator. Further R&D is required to address this issue.

Appendix D Resolution Function

Pinhole Geometry

The resolution function for momentum transfer $Q = 4\pi/\lambda \sin\theta$ consists of two parts:

$$(\delta Q/Q)^2 = (\delta\lambda/\lambda)^2 + \mathrm{ctg}^2\theta\ \delta\theta^2 \qquad (D.1)$$

where λ is the wavelength of neutrons and 2θ is the scattering angle. On a pulsed neutron source, the wavelength resolution is determined by the pulse width δt and the detector-to-source distance L:

$$(\delta\lambda/\lambda) = \delta t\ h/m/L = 3.956\ \delta t/L \qquad (D.2)$$

where δt is in [*ms*/Å] and L is in [m]. h is the Planck constant and m is the neutron mass.

For a pinhole set up, the standard deviation of the scattering angle in one dimension can be express as (Figure D1):

$$\delta\theta^2 = \tfrac{1}{4}\left[\delta o^2/L_s^2 + \delta s^2(1/L_s + 1/L_d)^2 + \delta d^2/L_d^2\right] \qquad (D.3)$$

where o,s, and d represent the source, the sample, and a detector pixel, respectively. L_s is the source-to-sample distance. L_d is the sample-to-detector distance. Combining (D.3) with (D.1), we get:

$$(\delta Q/Q)^2 = (\delta\lambda/\lambda)^2 + \tfrac{1}{4}\mathrm{ctg}^2\theta\ \left[\delta o^2/L_s^2 + \delta s^2(1/L_s + 1/L_d)^2 + \delta d^2/L_d^2\right] \qquad (D.4)$$

In two dimensions, the resolution function can be obtained through:

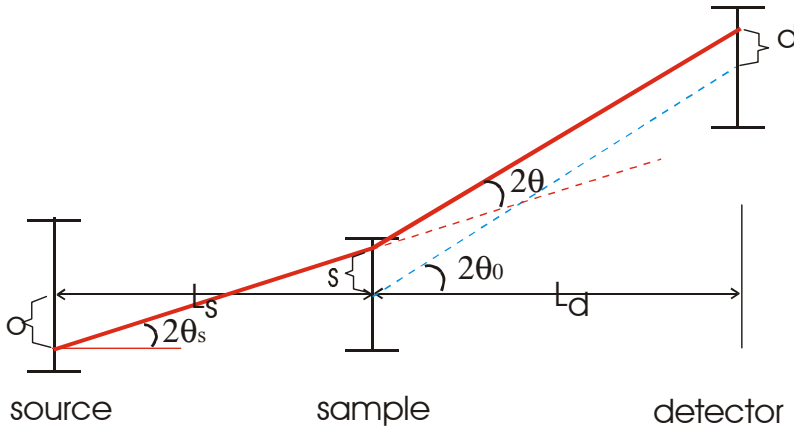

$$2\theta = 2\theta_0 + (d\text{-}s)/L_d - (s\text{-}o)/L_s$$

$$\delta\theta^2 = \tfrac{1}{4}\left(\delta o^2/L_s^2 + \delta s^2(1/L_s + 1/L_d)^2 + \delta d^2/L_d^2\right)$$

Figure D1. Angular resolution in one dimension. The red line represents the pathway of a neutron from position *o* on source to position *s* on sample, and detected at position *d* in a detector pixel.
Flat (square) flux distributions are assumed at the source, sample and the detector pixels. The full-width-half-max values for the source, sample and detector pixels are assumed to be their respective sizes. The standard deviations are assumed to be half these values.

$$\delta Q^2 = \delta Q_x^2 (Q_x/Q)^2 + \delta Q_y^2 (Q_y/Q)^2$$
$$= \tfrac{1}{2}\,\delta Q_x^2 + \tfrac{1}{2}\,\delta Q_y^2 \qquad \text{(D.5)}$$

where we have taken a circular average over the directions of the **Q** vector. If the source, sample and detector pixel all have square shape, then equation (D.5) reduces to the form of (D.4).

Soller Geometry

For Soller collimators converging onto the center of the detector (Figure D2),

$$\delta\theta^2 = \tfrac{1}{4}\,[\ \delta o^2/(L_1+L_2)^2 + \delta d^2/L_d^2 + \delta c_1^2 (L_c/L_1 L_d - 1/L1)^2 + \delta c_2^2 (1/L_d + L_c/L_1 L_d + 1/L_1)^2\ ] \qquad \text{(D.6)}$$

c_1 and c_2 are the entry and exit dimensions for one collimating channel, respectively. L_1 is the length of the collimator. L_d is the sample-to-detector distance. L_2 and L_c are the distances from the end of the collimator to the detector and sample, respectively.

For cross Soller collimators with separated x- and y- collimations, the resolution in the x- and y-directions are typically different because the channel dimensions are different in the two directions. However, since the source and sample apertures are almost always much larger than the width of a single channel, $\delta\theta$ is dominated by contributions from the apertures and the resolution difference between the x- and y-directions is minimal.

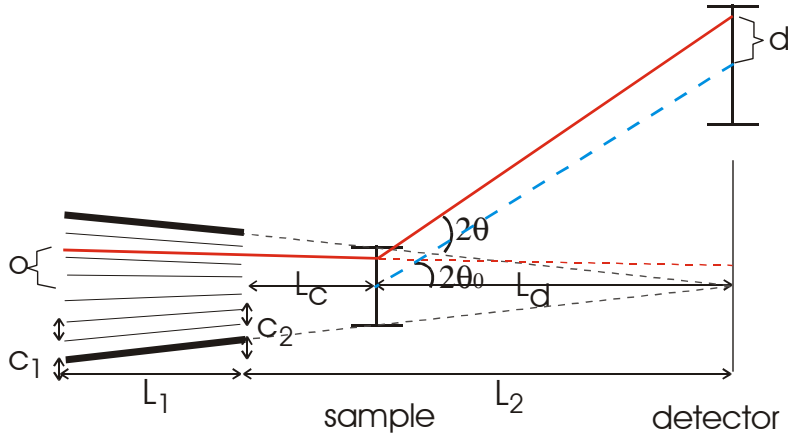

Visible sample size for one channel:

$$s' = c_2 + (c_1 + c_2)\ (L_c/L_1)$$

$$2\theta = 2\theta_0 + (d-s')/L_d - (c_2-c_1)/L_1 + o/(L_1+L_2)$$
$$= 2\theta_0 + d/L_d - c_2(1/L_d + L_c/(L_d L_1) + 1/L_1)$$
$$- c_1[L_c/(L_d L_1) - 1/L_1]$$
$$+ o/(L_1+L_2)$$

$$4\delta\theta^2 = \delta o^2/(L_1+L_2)^2 + \delta d^2/L_d^2$$
$$+ \delta c_1^2 (L_c/L_1 L_d - 1/L_1)^2 + \delta c_2^2 (1/L_d + L_c/L_1 L_d + 1/L_1)^2$$

Figure D2. Angular resolution for a Soller collimator converging onto the center of the detector. c_1 and c_2 are the entry and exit dimensions for one collimator channel. *o*,*c*, and *d* denote source, sample and one detector pixel, respectively.

Resolution on High Angle Detectors

For diffractions, the resolution function on high angle detectors can be expressed as δd/d, where d is the crystal d-spacing of the sample. From the Bragg's law 2d sinθ = λ,

$$(\delta d/d)^2 = (\delta\lambda/\lambda)^2 + \mathrm{ctg}^2\theta\ \delta\theta^2 \qquad \text{(D.7)}$$

Figure D3 shows the δd/d values assuming all detectors are 1m away from the sample. A better setting for diffraction applications is to arrange the detectors such that δd/d is constant. Figure 4 shows the required detector to sample distances for achieving 1.5%, uniform δd/d. Evidently, detectors at >50° can be located at shorter distances. However, closer than 1m will be neither practical nor necessary.

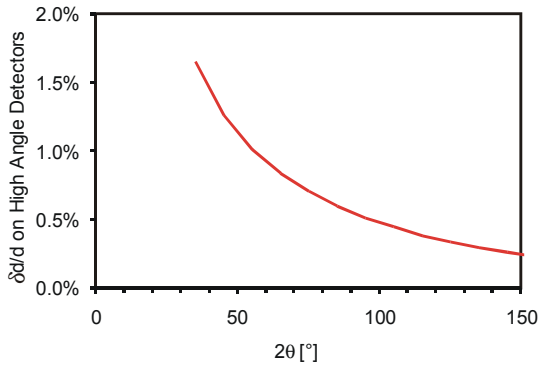

Figure D3. Resolution on high angle detectors 1m away from the sample. Calculation assumes 2 cm source size, 2m collimation length, 1 cm sample, and 0.5 cm detector pixels.

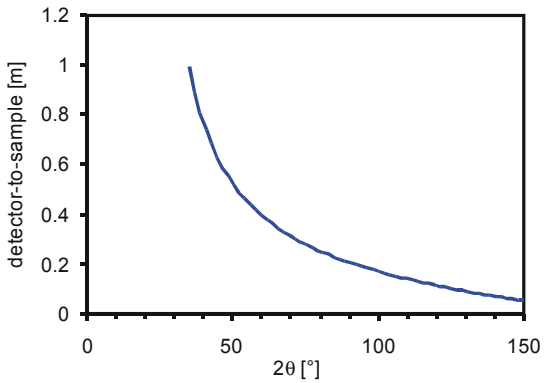

Figure D4. Required sample to detector distances for achieving a 1.5% δ*d*/*d*- resolution on all detectors. Parameters used for calculation are the same as in Figure D3.

Appendix E Monte-Carlo Simulation of the NIST 30m SANS on NG3

Simulations on the 30m SANS at NIST were performed to benchmark the simulation tools we have developed and used for simulating the Extended-Q SANS. The NG3 SANS parameters are obtained from Glinka et al (*J Appl. Cryst.* 1998 31,430-445, "*The 30m SANS at NIST*"). Supplementary technical details were obtained from Cook and Schroeder (Optical Filter for NG3 SANS, NIST report), Charlie Glinka (NIST, private communication) and Ralph Moon (HFIR/ORNL, private communication). The simulation conditions are as the following:

- The dimension of the NG3 instrument is as shown in Figure E1.
- ^{58}Ni and Ni coatings with 100% reflectivity were assumed for the guides (see Figure E1).
- 80%,75%, and 70% crystal filter transmission were used for 10Å,7.5 Å, and 5 Å neutrons, respecitvely. The value for 7.5Å was interpolated from the two published numbers for 5 and 10Å neutrons.
- Gaussian shaped transmitting curve was assumed for the velocity selector, with $\delta\lambda/\lambda$ = 15% (FWHM) and 70% transmission.
- The diameters of the sample and source apertures, as were used in Glinka et al, were 1.9cm and 3.8cm for configurations with no (moveable) guides and 2.5cm and 5cm for otherwise.

The simulated fluxes at the sample position are shown in Figure E2. They are within a factor of ~2 of the reported numbers (table 1 in main text). The difference can be attributed to many factors, such as surface roughness, surface flatness and alignment of the guides; and window materials in neutron flight path. Since the Extended-Q SANS has only 14m of primary flight path, as opposed to ~49m on the NIST 30m SANS, we believe the estimated performances on the Extended-Q SANS presented in this document should be accurate within the factor of 2.

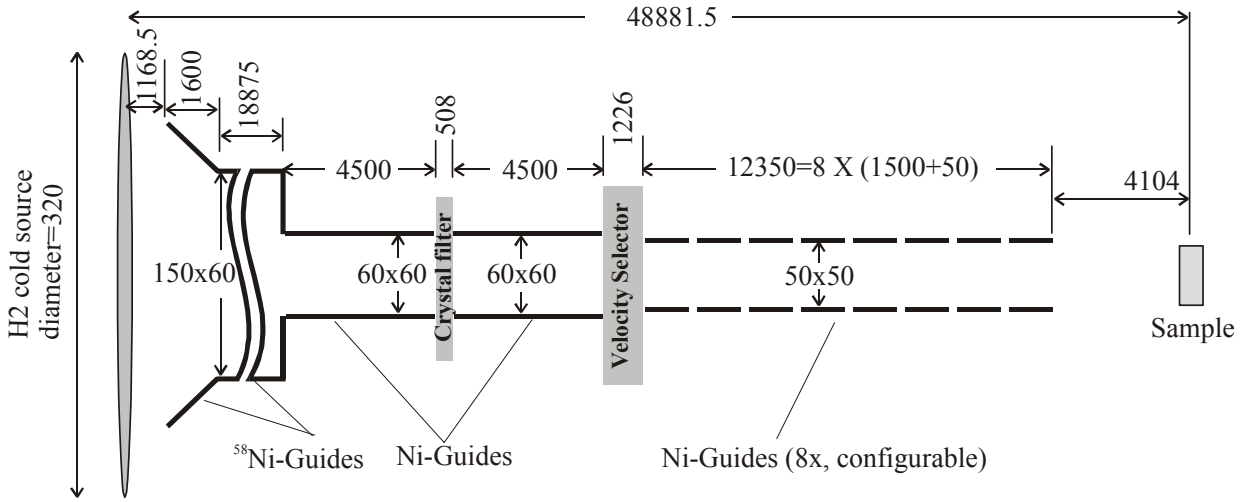

Figure E1. NG3-SANS setup used for Monte-Carlo Simulations. The dimensions are in *mm*.

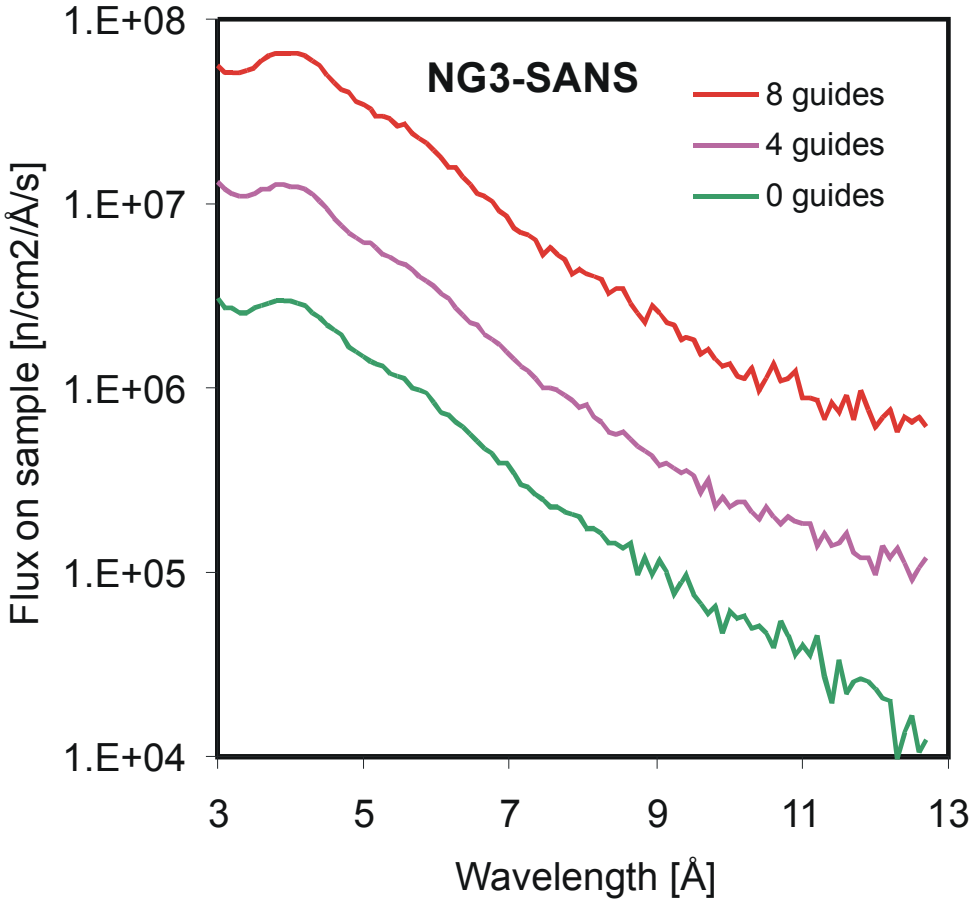

Figure E2 Simulated Fluxes on the NG3 SANS at NIST with the crystal filter and velocity selector not in the beam. The statistics corresponds to 0.7, 3,and 15 ms data collection times for configurations with 8,4 and 0 guides, respectively.

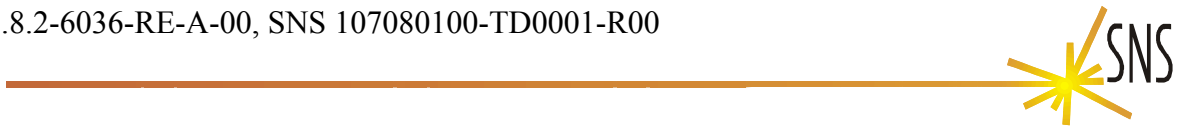

Acknowledgements

The author is very thankful to many friends and collegues who have offered their warm supports in designing the SANS instrument and preparing this document. Especially, the author would like to acknowledge the spokespersons of the SANS Instrument Advisory Team - Prof. B. Heuser of UIUC and Prof. S-H.Chen of MIT; Dr. R. Heenan of ISIS; and Drs P. Thiyagarajan and K. Crawford of IPNS.